

Synthesis Of A New Family Of Non Ion Surfactants And Evaluation Of Their Performance As Corrosion And Scale Inhibitors For Copper In Desalination Water Plants

M. A. Migahed^a, A. A. Misbah, A. H. Marei, M. Abd-El-Raouf^{*}, S. B. Mahmoud^b

^a*Egyptian Petroleum Research Institute (EPRI), Nasr city, Cairo 11727, Egypt*

^b*Chemistry department, Faculty of Girls for Arts, Science and Education, Ain Shams
University, Cairo, Egypt*

(Corresponding author: abdelraouf1979@yahoo.com)

Abstract

Corrosion of metallic surfaces and formation of mineral scales are significant problems in cooling water systems. Corrosion process causes a great deterioration of metallic surface, while scale deposition decreases the efficiency of heat exchange. So that, these phenomena have a great economic impact. In this work, a new family of non ionic surfactants based on acrylic acid was synthesized to evaluate their performance as corrosion and scale inhibitors for copper alloy in sea water by various techniques such as weight loss, potentiodynamic polarization and electrochemical impedance spectroscopy (EIS). The results showed the selected compound act as a very good scale and corrosion inhibitors. Finally, the effect of addition of the synthesized acrylic acid derivatives on CaSO_4 crystals formation was examined by SEM and EDX techniques.

Key words Scale and corrosion inhibitors, Non ionic surfactants, Desalination water plants, CaSO_4 crystals formation, EDX, SEM .

Introduction

Water used in industrial cooling water system which comes from rivers, lakes, or from underground reservoirs. [1]. such water contains dissolved inorganic salt such as Ca^{2+} , Mg^{2+} ; etc. It is well known that, Copper has excellent electrical and thermal conductivities in addition to their high mechanical workability. So that, it is widely used in heating and cooling systems. Scales and corrosion products have negative influence on heat transfer efficiency [2]. Thus, corrosion of copper and copper

alloys and their inhibition in aqueous salt solutions have attracted the attention of a number of investigators [3–8]. Scale can be defined as an adherent deposit of inorganic compounds which formed by precipitation of salts from water and crystal growth on heat transfer surface. As the salts precipitation on the internal surface of cooling system, they inhibit effective heat transfer, restrict the flow of the water, and promote the development of under deposit corrosion [9]. Scale formation is controlled by altering a system design, acidification of circulating water, lime softening and demineralization, use of chelating chemicals and threshold inhibitors. [10-11]. The use of naturally occurring polymers and chelating chemicals is limited due to their instability at higher temperature and need of large amount of chemicals respectively [12]. The use of inorganic or organic inhibitors is one of the most practical methods for protection against corrosion of metals and their alloys. Most well-known organic inhibitors such as those containing nitrogen, sulfur, oxygen atoms and aromatic rings [13–17]. To be effective, an inhibitor must displace water molecules from the metal surface, interact with anodic and/or cathodic reaction sites to retard the partial oxidation and reduction corrosion reaction and prevent transportation of water and corrosive-active species to the surface [18,19]. The present work aims to study the effectiveness of a new family of non ionic surfactants based on acrylic acid as corrosion and scale inhibitor for copper alloy in desalination water plants.

2. Experimental

2.1. Chemical composition of the investigated copper alloy

Copper specimens used in this investigation were cut from unused petroleum pipeline as regular edged cuboids with dimensions $2 \times 1 \times 0.1$ cm. The chemical composition of copper was listed in (Table 1).

2.2 Sea Water:

The sea water which used in this study from Mediterranean Sea in Alex. The chemical composition of the seawater was listed (Table 2)

2.3. Synthesis of the inhibitors

Acrylic acid (2 mole) was added to (1 mole) of ethylene diamine in three necked round bottomed flask equipped with a mechanical stirrer, condenser and a thermometer. The reaction mixture was heated to $155\text{ }^{\circ}\text{C}$ until the theoretical amount of water has been collected using a Dean Stark apparatus. The obtained intermediate reacts with (40 mole) of ethylene oxide to give the inhibitor (I) and by the same way prepare inhibitors (II and III) by added di ethylene tri amine and tri ethylene tetraamine respectively showed in scheme 1

The synthesized structures were identified by ^1H NMR and IR spectroscopic analyses as shown in Fig. 1 & 2.

2.4. Weight loss measurements

The specimens were polished with different grade emery papers, degreased with hot acetone [23]. Then washed with bi-distilled water and finally dried. The weight losses

(mg cm⁻²) of rectangular copper alloy specimens in seawater in the absence and presence of various concentrations of the inhibitors were determined. Triplicate specimens were exposed to each condition and the mean weight loss was reported.

2.5. Open circuit potential:

The potential of copper alloy electrode was measured against saturated calomel electrode (SCE) in sea water in the absence and presence of different concentrations of each inhibitor. All measurements were carried out using Volta lab 80 (Tacussel-radiometer PGZ 402)

2.6. Potentiodynamic polarization measurements

The electrochemical measurements were carried out using Voltalab80 (Tacussel-radiometer PGZ402) controlled by Tacussel corrosion analysis software model (Volta master 4). A platinum electrode was used as auxiliary electrode. All potentials were measured against a saturated calomel electrode (SCE) as a reference electrode.

2.7. Electrochemical impedance spectroscopy (EIS)

Electrochemical impedance (EIS) measurements were carried out using Volta lab 80 potentiostat (Tacussel-radiometer PGZ402) controlled by Tacussel corrosion analysis software model (Volta master 4). Impedance spectra were obtained in the frequency range between 100 KHz and 50 mHz using 20 steps per frequency decade at open circuit potential after 1 h of immersion time. AC signal with 20 mV amplitude peak to peak was used to perturb the system. EIS diagrams are given in both Nyquist and Bode representations

2.8. Evaluation of acrylic acid derivatives as scale inhibitors for calcium sulfate deposition:

Experimental procedure involves dissolving 9.11g of CaCl₂ per L of double distilled water (brine A). on the other hand the sulfate solution (brine B) can be prepared by dissolving 7.3 g of Na₂SO₄ per L of double distilled water .test protocol consists of mixing 50 ml of calcium solution to 50 ml of sulfate solution. The solutions are then incubated in water thermostat at 90 C for 24 hours. At the end of test duration, the solution is filtered through a 0.22-micron filter paper and the calcium concentration is analyzed by titration using 0.01 M EDTA and Murexide as indicator. Experimental were reported for different doses (25-125 ppm) of inhibitor at the same test duration

2.9. Surface tension measurements

The surface tension (c) was measured using (Kruss K6 Tensiometer type, a direct surface tension measurement using ring method) for various concentrations of the investigated inhibitors.

2.10. Scanning electron microscopy

The surface examination was carried out using scanning electron microscope (JEOL JSM-5410, Japan). The energy of the acceleration beam employed was 20 KV. All micrographs were taken at a magnification power (X 750).

2.11. Energy dispersive analysis of X-rays (EDX)

EDX system attached with a JEOL JSM-5410 scanning electron microscope was used for elemental analysis or chemical

3. Results and discussion

3.1. Weight loss measurements

Figs. 3 and 4 show the variation of both corrosion rate against concentration and the percentage inhibition efficiency against concentration curves for copper alloy immersed in sea water in the absence and presence of various concentrations of the inhibitor (III) as a representative sample. It is apparent that, increasing inhibitor concentration was accompanied by a decrease in corrosion rate. This behavior can be attributed to the adsorption of surfactant molecules on copper alloy. And by increasing concentration of inhibitors the efficiency increase. The maximum inhibition efficiency (η %) was exhibited at 500 ppm concentration of the inhibitor. The degree of surface coverage (θ) and percentage inhibition efficiency (η %) were calculated from the following equations:

$$\theta = (W_o - W / W_o) \quad (1)$$

$$\eta (\%) = (W_o - W / W_o) \times 100 \quad (2)$$

Where, w_o and w . represent the values of weight loss of copper alloy in seawater in the absence and presence of the inhibitor, respectively.

Corrosion rate was calculated using the following equation [24, 25]:

$$mpy = \frac{\Delta W \times 3.45 \times 10^6}{A \times T \times d} \quad (3)$$

Where, $K = 3.45 \times 10^6$, T is the exposure time in hour, A is the surface area of the test specimen, W is the weight loss in gram and D is the density of the test specimen in g/cm^3 , respectively. Complete data are summarized and listed in Table 3

3.2. Open circuit potential measurements (OCP)

The potential of the copper electrodes immersed in the sea water were measured as a function of immersion time in the absence and presence of different concentrations of synthesized inhibitors. The obtained potential – time curves are shown in Figs. (5). All measurements were carried out until the steady state potentials are attained. The steady state represents an equilibrium state at which oxidation current density (I_{ox}) equal to reduction current density (I_{red}). It is clear that the potential of the copper electrode immersed in sea water (blank curve) tends toward more negative potential firstly, giving rise to short step. Addition of inhibitor molecules to the aggressive medium produces a slightly positive shift in the corrosion potential E_{corr} due to the formation of a protective film

3.3. Potentiodynamic polarization measurements

Figs. 6 and 7 show the cathodic and anodic polarization curves of copper alloy immersed in sea water in the absence and presence of various concentrations of the inhibitor (III) as a representative sample. Electrochemical parameters such as corrosion potential (E_{corr}), corrosion current density (i_{corr}), cathodic and anodic Tafel

slopes (b_c and b_a) and polarization resistance (R_p) were calculated. From the obtained polarization curves, it is clear that the corrosion current densities (i_{corr}) were decreased with increasing concentration of inhibitor (III) with respect to the blank (inhibitor free solution). These results greatly agree with the previous data obtained from weight loss measurements and confirm the formation of a good protective layer on the surface of copper alloy. The degree of surface coverage (θ) and the percentage inhibition efficiency ($\eta\%$) were calculated using the following equations [26]:

$$= i - \frac{i}{i_0} \quad (4)$$

$$\eta\% = \left(i - \frac{i}{i_0}\right) \times 100 \quad (5)$$

where i_0 and i are the corrosion current densities in the absence and presence of the inhibitor, respectively.

The values of polarization resistance (R_p) were calculated from the well-known Stern–Geary equation:

$$R_p = \frac{b_a b_c}{2.303 i_{\text{corr}} (b_a + b_c)} \quad (6)$$

From the obtained data, it is clear that Tafel lines are shifted to more negative and more positive potentials for the anodic and cathodic processes, respectively relative to the blank curve. This means that the selected compound acts as mixed type inhibitor, i.e., promoting retardation of both anodic and cathodic discharge reactions. Also, the slopes of the cathodic and anodic Tafel lines are approximately constant and independent on the inhibitor concentration. This means that, the selected inhibitor has no effect on the metal dissolution mechanism. Complete data obtained from polarization measurements are summarized and listed in Table 4. The results indicate that the percentage inhibition efficiency ($\eta\%$) of the inhibitor (III) is greater than that of inhibitors (I and II). This could be attributed to the increase of inhibitor which promotes stronger adsorption on metallic surface forming a good protective film.

3.4. Electrochemical impedance spectroscopy (EIS)

The corrosion behavior of copper alloy in sea water in the absence and presence of various concentrations of inhibitor (III) as a representative sample was investigated by EIS technique. Nyquist and Bode plots are shown in Figs. 8 and 9. It is clear from the plots that the impedance response of copper alloy in sea water was significantly changed after the addition of the inhibitor molecules. Various parameters such as the charge transfer resistance (R_t), double layer capacitance (C_{dl}) and percentage inhibition efficiency $\eta\%$ were calculated according to the following equations and listed in Table 5.

The values of R_t were given by subtracting the high frequency impedance from the low frequency one as follows [27]:

$$R_t = Z_{\text{re}}(\text{at low frequency}) - Z_{\text{re}}(\text{at high frequency}) \quad (7)$$

The values of C_{dl} were obtained at the frequency f_{max} , at which the imaginary component of the impedance is maximal – Z_{max} using the following equation:

$$C_{dl} = \frac{1}{2\pi f Z_{im} \max} \frac{1}{R_t} \quad (8)$$

The percentage inhibition efficiency η , IE% was calculated from the values of R_t using the following equation:

$$\eta\% = \frac{R_t(inh) - R_t}{R_t(inh)} \quad (9)$$

where R_t and $R_t(inh)$ are the charge transfer resistance values in the absence and presence of inhibitor, respectively. Increasing the value of charge transfer resistance (R_t) and decreasing the value of double layer capacitance (C_{dl}) by increasing the inhibitor concentration indicate that the surfactant molecules inhibit corrosion rate of copper in sea water by adsorption mechanism [28]. From EIS data it was found that the percentage inhibition efficiency of inhibitor (III) is greater than that of inhibitors (I and II) thereby, agreeing with aforementioned results of weight loss and potentiodynamic polarization measurements

3.5 Evaluation of acrylic acid derivatives as scale inhibitors

The present work was extended to establish the effectiveness of acrylic acid derivatives as scale inhibitor for calcium sulfate deposition in synthetic cooling water. The laboratory procedures were carried out as described in the experimental part. The percentage inhibition efficiency was calculated as follow:

$$\text{Scale inhibition efficiency \%} = (C_{ai} - C_{ab} \setminus C_{ac} - C_{ab}) \times 100 \quad (10)$$

Where C_{ai} = Calcium ion concentration for the sample treated with the inhibitor after precipitation

C_{ab} = Calcium ion concentration in the blank solution after precipitation

C_{ac} = Calcium ion concentration in the blank solution before precipitation

The obtained results are listed in table (6) and graphically shown in fig.(10) it is clear that the percentage inhibition efficiency increase by increasing the inhibitor, reaching 90% at 125 ppm.

3.6. Surface tension measurements

The values of surface tension (γ) were measured at various concentrations of the inhibitors (I, II and III). The measured values of (γ) were plotted against logarithm of surfactant concentration; $\log C$, as shown in Fig. 11. These plots indicate that each surfactant is molecularly dispersed at low concentration, leading to a reduction in surface tension until certain concentration is reached the surfactant molecules form micelles, which are in equilibrium with the free surfactant molecules. The intercept of the two straight lines designates the critical micelle concentration (cmc), where saturation in the surface adsorbed layer takes place. The surface active properties of the surfactants (I, II and III); effectiveness (γ_{cmc}), maximum surface excess (Γ_{max}) and minimum area per molecule (A_{min}) were calculated using the following eq. [13]:

$$\pi_{cmc} = \gamma_0 - \gamma_{cmc} \quad (11)$$

$$\Gamma_{max} = \frac{-1}{RT[\partial\gamma/\partial\ln C]_T} \quad (12)$$

$$A_{min} = \frac{1}{\Gamma_{max} \times NA} \quad (13)$$

Where γ_0 is the surface tension of pure water, γ_{cmc} the surface tension at critical micelle concentration and NA is the Avogadro's number. The data obtained from surface tension measurements were summarized and presented in Table 11.

The critical micelle concentration (CMC) considers a key factor in determining the effectiveness of surfactants as corrosion inhibitors [29]. Below the CMC, as the surfactant concentration increases, the surfactant molecules tend to adsorb on the metal surface, leading to increase the inhibition efficiency of the surfactant. On the other hand, increasing the surfactant concentration above CMC does not affect the surface tension, which is, in turn, does not influence the value of inhibition efficiency. This could be attributed to the fact that above CMC the surface of copper is covered with a monolayer of surfactant molecules and the additional molecules combine to form micelles in the bulk of solution. It has to be noted that for a surfactant to be an excellent corrosion inhibitor it should exhibit a low CMC value, since the inhibition effectiveness decreases as the CMC value increases. On the basis of this view, among all the studied compounds, the surfactant (III) which shows the lowest CMC value and hence it considers the most effective corrosion inhibitor for copper in sea water.

3.7. Scanning electron microscopy (SEM)

Fig. 12a shows SEM image of calcium sulfate scale in the absence and presence of acrylic acid derivative. It is clear from these images that the presence of 125 ppm of acrylic acid derivative in the synthetic cooling water minimize the deposition of large amounts of calcium sulfate. (30), because, it has a crystal distortion effect and a threshold effect (31). by this way, the acrylic acid derivative molecules can be adsorbed on copper surface, imparting it alike charge and thereby causing the particles to remain in suspension, because of charge repulsion. In addition, the polymer can distort scale crystals by disruption their lattice structure and normal growth patterns. The inclusion of relatively large irregularly shaped polymer in the scale lattice tends to prevent the deposition of a dense uniformly structured crystalline mass on the metal surface.

3.8. Energy dispersive analysis of X-rays (EDX)

The EDX spectrum in Fig. 13a shows the characteristic peaks of some of the elements constituting the polished copper surface. The spectrum of the polished copper surface after immersion in the sea water in the absence and presence of inhibitor (III) for 7 days, is shown in Figs. 16b and c), respectively. The spectrum of Fig. 16c shows that the Cu peak is considerably decreased relative to the samples in Figs. 16a and b). This decreasing of the Cu band is indicated that strongly adherent protective film of inhibitor (V) formed on the polished copper surface, which leads to a high degree of inhibition efficiency [32]. The oxygen signal apparent in Fig. 16b is due to the copper surface exposed to the sea water in the absence of inhibitor (V). Therefore, the EDX and SEM examinations of the copper surface support the results obtained from the chemical and electrochemical methods that the synthesized surfactant inhibitors are

good inhibitors for the copper in the sea water.

Conclusion:

- The synthesized compounds act as good corrosion and scale inhibitors for copper in sea water that used in cooling water systems.
- Potentiodynamic polarization showed that the selected compound suppresses both anodic and cathodic process, this means that the selected compound acts as mixed type inhibitor.
- The high scale inhibition efficiency can be attributed to the ability of acrylic acid derivatives to distort scale crystals by disrupting their lattice structure and normal growth patterns.
- The inhibition mechanism is attributed to the strong adsorption ability of the synthesized compounds on copper surface. Forming a good protective layer, which isolates the surface from the aggressive environment as seen from SEM and EDX technique.
- The critical micelle concentration considers a key factor in determining the effectiveness of surfactants as corrosion inhibitors due to large reduction of surface tension at CMC.
- By increasing concentration of inhibitors R_t was increased while C_{dl} was decreased.

Table 1: Chemical composition of copper alloy

	Chemical composition,% (weight)										
	Cu+Ag	Bi	Sb	As	Fe	Ni	Pb	Sn	S	Zn	O
Max	99.90	—	—	—	—	—	—	—	—	—	—
Min	-	0.001	0.002	0.002	0.005	—	0.005	—	0.005	—	—

Table 2: Chemical composition of Sea water used in this investigation.

Component	Concentration mg/L (or ppm)	Component	Concentration mg/L (or ppm)
Cl^-	18.980	H_3BO_3	26
Na^+	10.556	Sr^{+2}	13
SO_4^{-2}	2.648	F^-	1.3
Mg^{+2}	1.272	I^-	0.05
Ca^{+2}	400	Si	4.0 to 0.02
K^+	380	Other	1.3
HCO_3^-	139	H₂O	965.517
Br^-	64	Total	1.000.000

Table 3: weight loss data obtained for copper alloy immersed in seawater in absence and presence of various concentrations of inhibitor (I, II and III) .

Inhibitor	Concentration, (ppm)	Corrosion rate, (mpy)	Surface Coverage (θ)	Inhibition Efficiency η %
Blank		1.33	-	-
Inhibitor I	50	1.12	0.791	55
	100	1.04	0.735	57
	200	0.93	0.656	59
	300	0.85	0.595	65
	400	0.83	0.573	73
	500	0.80	0.559	79
Inhibitor II	50	1.20	0.658	65.8
	100	1.12	0.633	63.3
	200	0.99	0.654	65.4
	300	0.93	0.698	69.8
	400	0.91	0.796	79.6
	500	0.93	0.857	85.7
Inhibitor III	50	1.28	0.577	57.7
	100	1.20	0.616	61.6
	200	1.07	0.693	69.3
	300	0.99	0.754	75.4
	400	0.88	0.854	85.4
	500	0.83	0.912	91.2

Table 4: Data obtained from potentiodynamic polarization measurements of copper alloy immersed in sea water in the absence and presence of various concentrations of the inhibitors (I, II and III) .

Inhibitor	Conc, (ppm)	R _p , (k ohm cm ⁻²)	I _{corr} , (mA cm ⁻²)	E _{corr} , (mV vs SCE)	b _c , (mV dec ⁻¹)	b _a , (mV dec ⁻¹)	□ %
	Blank	7	48	-350	-273	88	
Inhibitor I	50	7.3	28	-353	-271	88.3	41.6
	100	9.1	25.7	-352	-264	95.5	46.4
	200	10.78	24.1	-342	-254	106	49.7
	300	10.49	19.3	-339	-251	94.1	59.7
	400	11.56	16	-337	-240	93.7	66.6
	500	14.60	12	-318	-233	108.9	75
Inhibitor II	50	1.1	18.2	-469	-289	131	62.0
	100	1.24	13.3	-429	-253	214	72.2
	200	2.44	13	-427	-247	242	72.9

	300	2.96	12.6	-408	-196	369	73.7
	400	4.26	11.1	-396	-187	185	76.8
	500	4.55	4.6	-373	-172	242	90.4
Inhibitor III	50	1.6	8.7	-414	-243	279	81.8
	100	1.7	5.7	-399	-241	262	88.1
	200	1.8	4.9	-365	-233	222	89.7
	300	2.4	4.3	-354	-211	221	91
	400	2.7	4.2	-343	-197	208	91.2
	500	3	3.2	-333	-188	200	93.3

Table 5: Data obtained from electrochemical impedance spectroscopy (EIS) measurements of copper in sea water solution in absence and presence of various concentrations of the inhibitors (I, II and III).

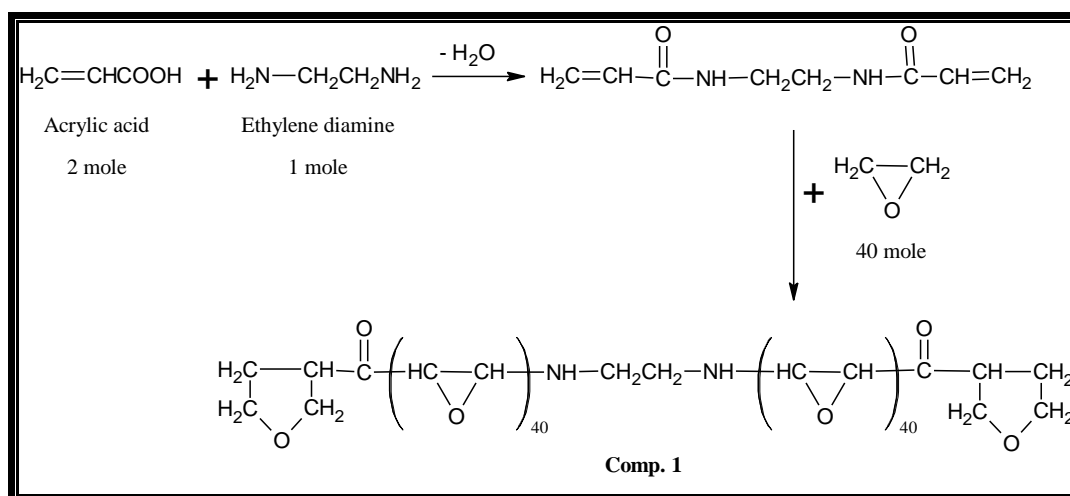
Inhibitor	Concentration (ppm)	R_t, (ohm cm⁻²)	C_{dl} (mF cm⁻²)	η %
	Blank	0.55	3.3	-
Inhibitor I	50	3	7.8	81.6
	100	3.7	6.9	85.1
	200	4.5	6.8	87.7
	300	4.9	6.4	88.7
	400	5.2	3.9	89.4
	500	5.9	2.8	90.6
Inhibitor II	50	4	7.7	86.2
	100	5.02	5.1	89.0
	200	6.18	4.7	91.1
	300	6.3	4.6	91.2
	400	6.4	2.8	91.4
	500	6.7	1.4	91.7
Inhibitor III	50	4.54	9.6	87.8
	100	5.2	9.3	89.4
	200	5.6	7.8	90.1
	300	5.7	5.5	90.3
	400	6.4	4.4	91.4
	500	7	3.8	92.1

Table 6: Percentage inhibition efficiency of (inhibitor I, II and III) of acrylic acid derivative as calcium sulfate scale inhibitor at various concentrations.

concentration of the inhibitors, ppm	Blank	25	50	75	100	125
η % Inhibition efficiency of compound I	-	47.5	55.1	62.5	70.5	75.3
η % Inhibition efficiency of compound % II	-	67.5	77.5	80.3	82.5	85.2
η % Inhibition efficiency of compound % III	-	65.6	72.5	80.1	85.5	90.2

Table 7: Surface active properties of the three synthesized inhibitors (I, II, and III).

Surfactants	CMC, (mmol/l)	γ_{cmc} , (mN/m)	Π_{cmc} , (mN/m)	$\Gamma_{max} \times 10^{10}$ (mol/cm ²)	A _{min} (nm ²) $\times 10^2$
Inhibitor I	2.9$\times 10^{-4}$	36	38	7.5	0.23
Inhibitor II	4.6$\times 10^{-5}$	42	32	7.3	0.23
Inhibitor III	3.6$\times 10^{-4}$	42	32	7	0.24



Scheme 1: Synthesis of Inhibitors

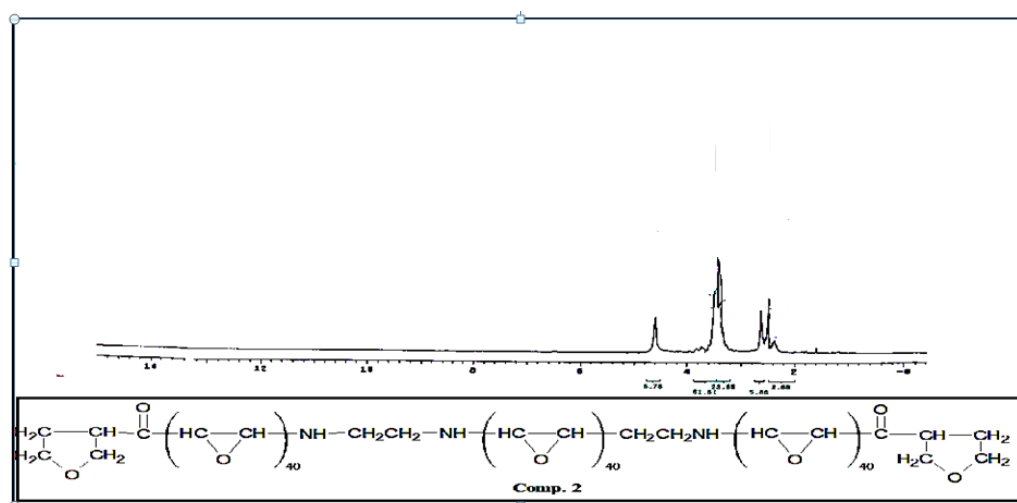


Figure 1H NMR spectrum of inhibitor (II)

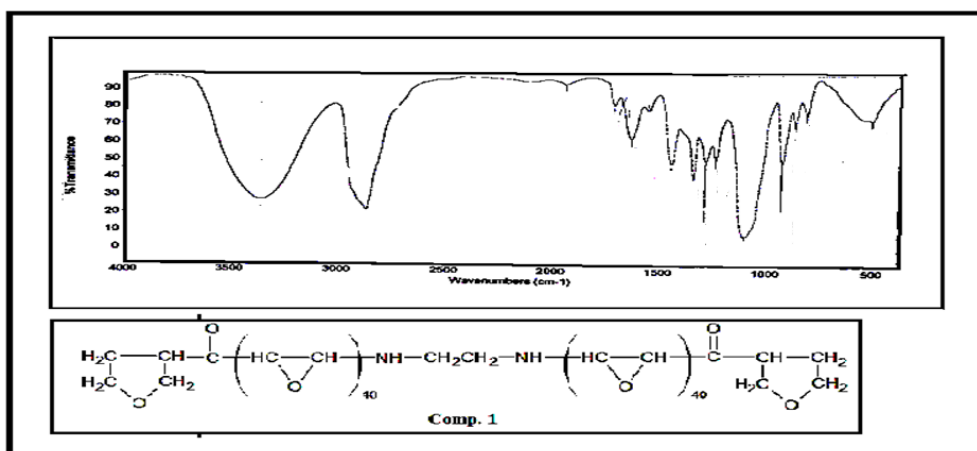


Figure 2 FTIR spectrum of inhibitor (II).

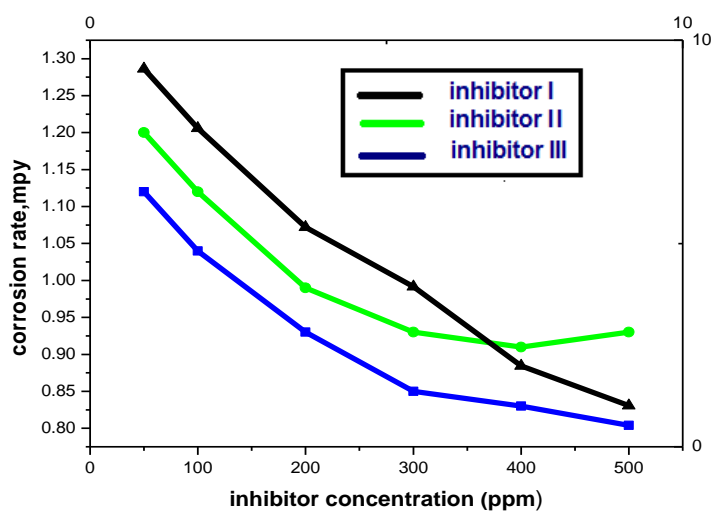


Fig. 3 Relationship between the copper corrosion rate and inhibitors concentrations for all inhibitor (I-III) for copper dissolution in sea water as obtained from weight loss technique.

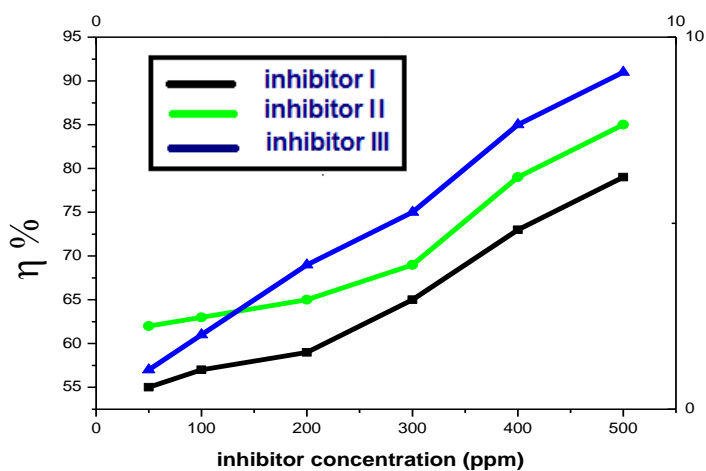


Fig.4 Relationship between the inhibition efficiency and inhibitors concentration for all inhibitor (I-III)for copper dissolution in sea water as obtained from weight loss technique.

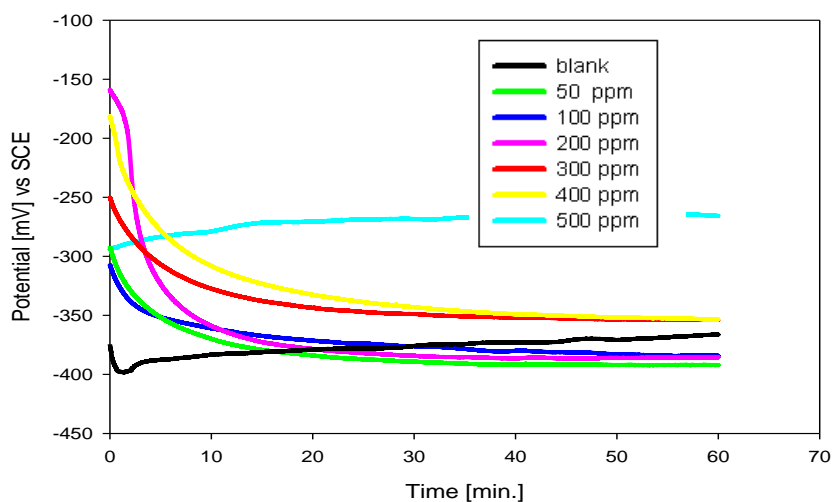


Fig.5 Potential–time curves for copper in sea water in the absence and presence of various concentrations of the inhibitor (III) at 303

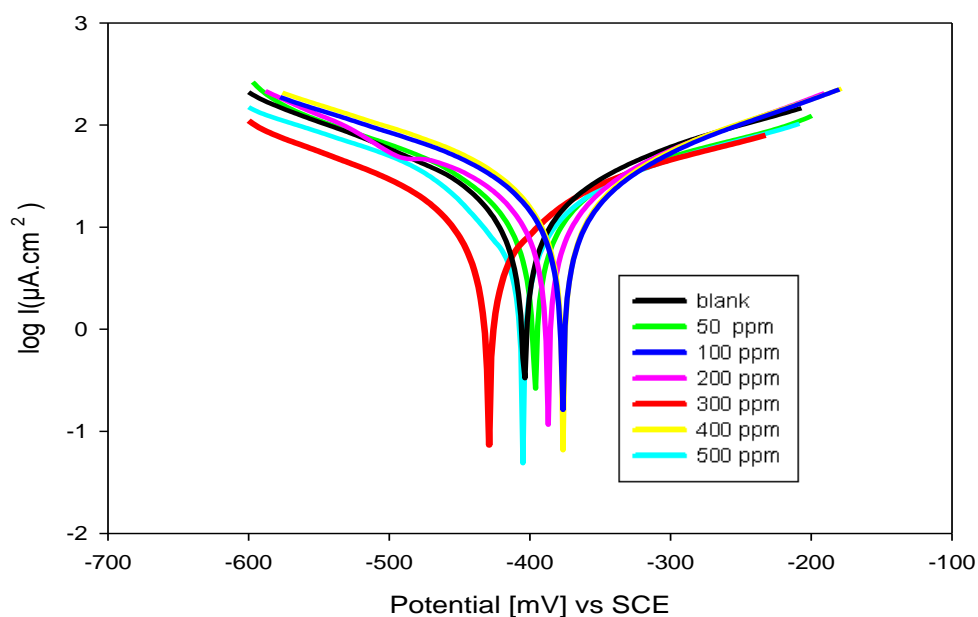


Fig 6 Potentiodynamic polarization curves (E – $\log I$ relationship) of copper in sea water in the absence and presence of different concentrations of the inhibitor (III).

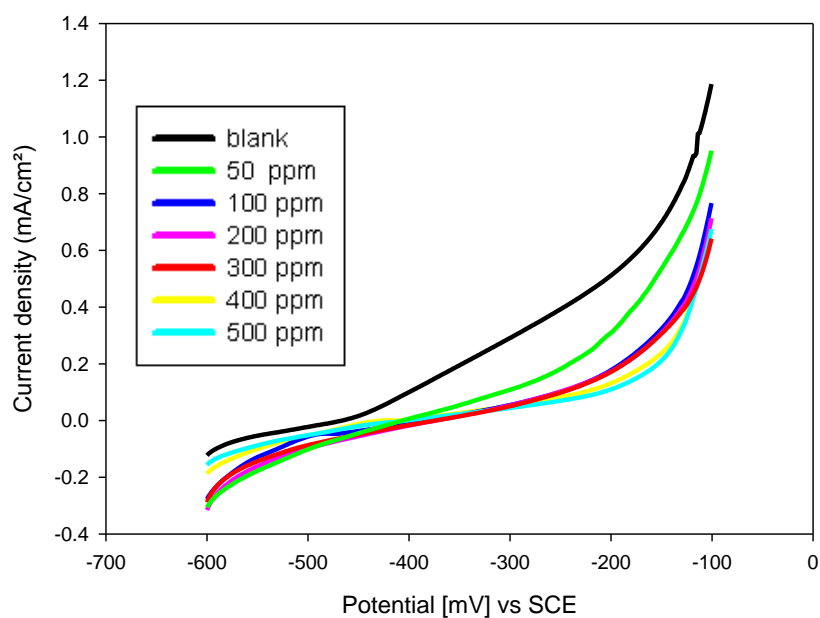


Fig. 7 Potentiodynamic polarization curves (E – I relationship) of copper in sea water in the absence and presence of different concentrations of the inhibitor (III).

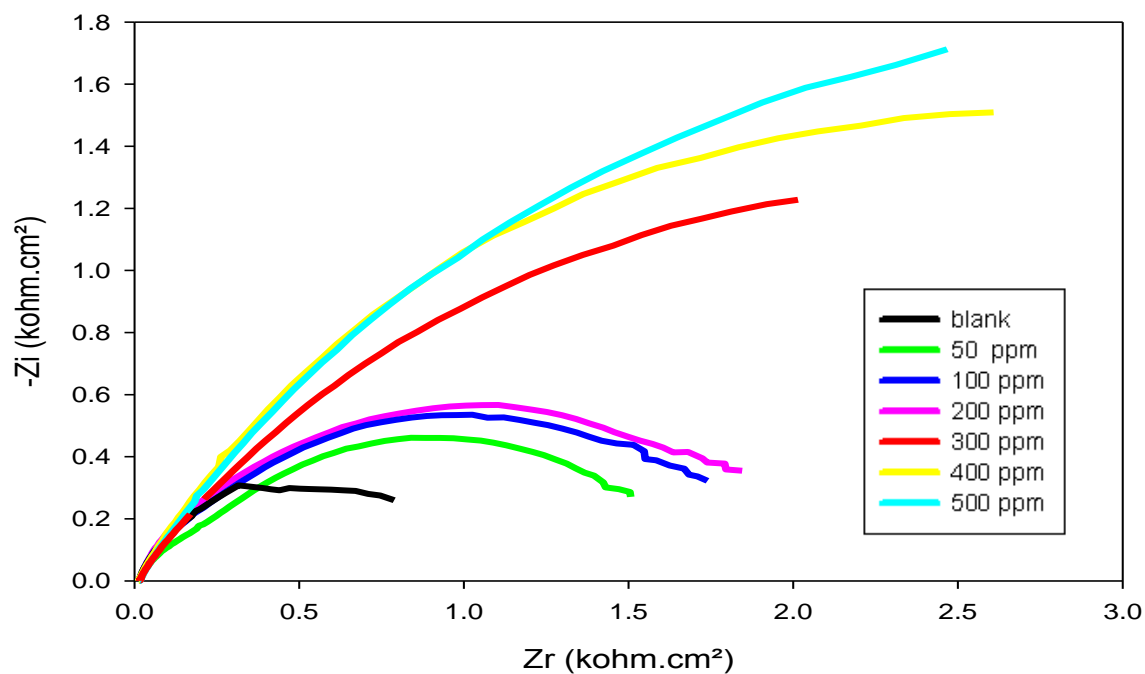


Fig. 8 Nyquist plots for copper in sea water in the absence and presence of various concentrations of inhibitors (III)

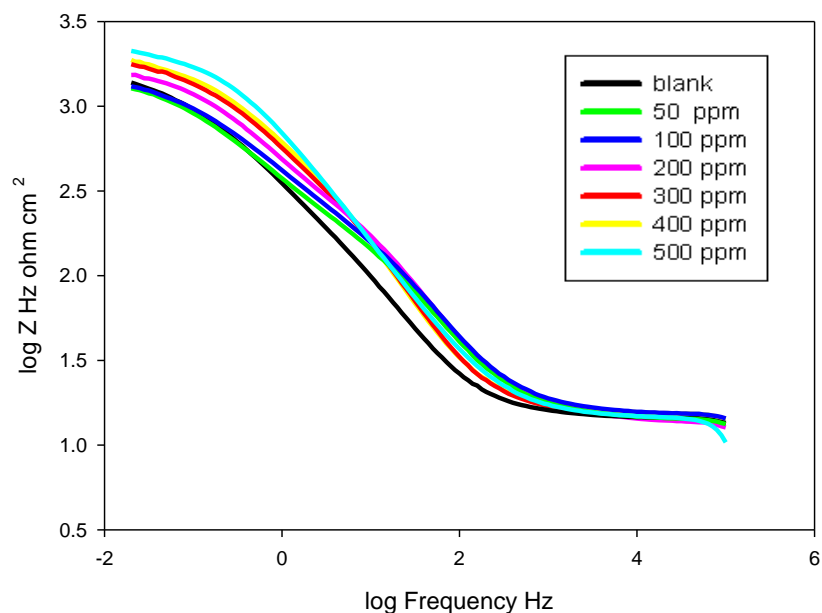


Fig. 9 Bode plots (Z–logZ relationship) of carbon steel in formation water in the absence and presence of various concentrations of the inhibitor (III).

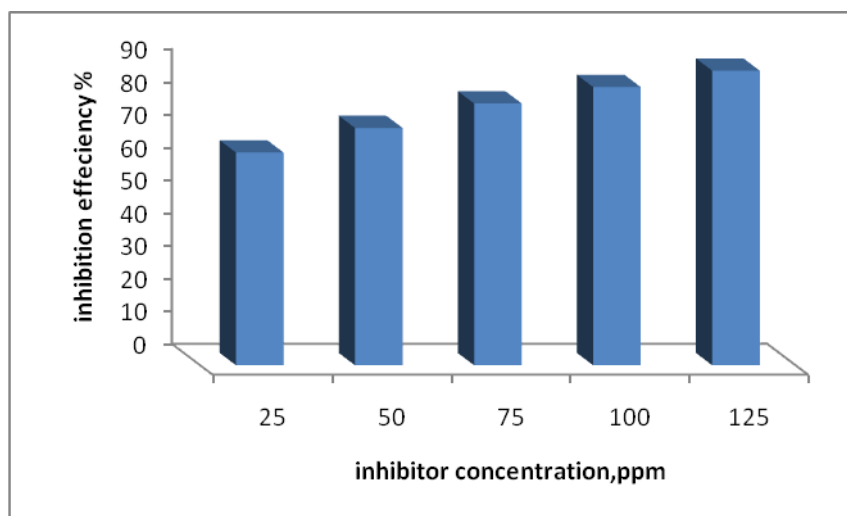
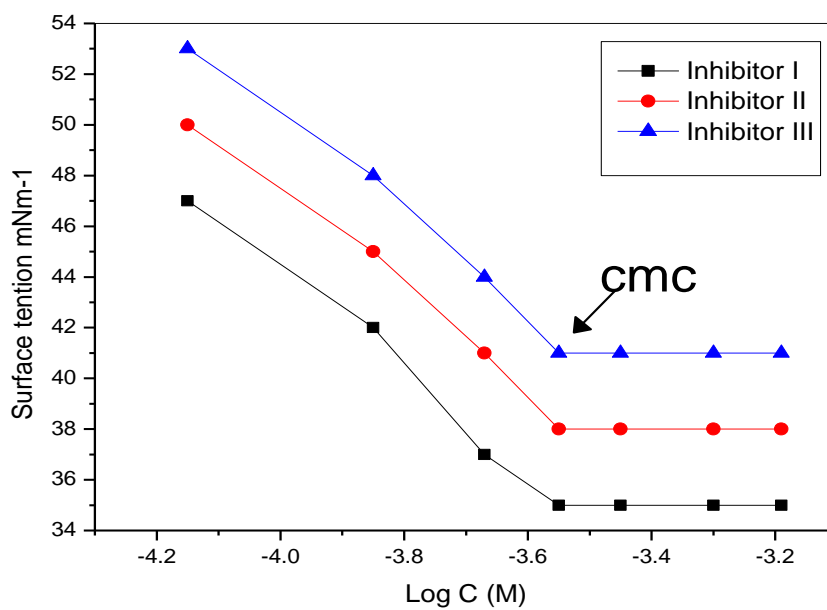


Fig.10 Effect of inhibitor (III) concentration on scale inhibitorefficiency of calcium sulfate deposition in copper surface as calculated from complex metric titration measurements.



ig.11 Surface tension (γ) vs. $\log C$ at different concentrations of the inhibitor (I, II, and III) at 303 K. **F**

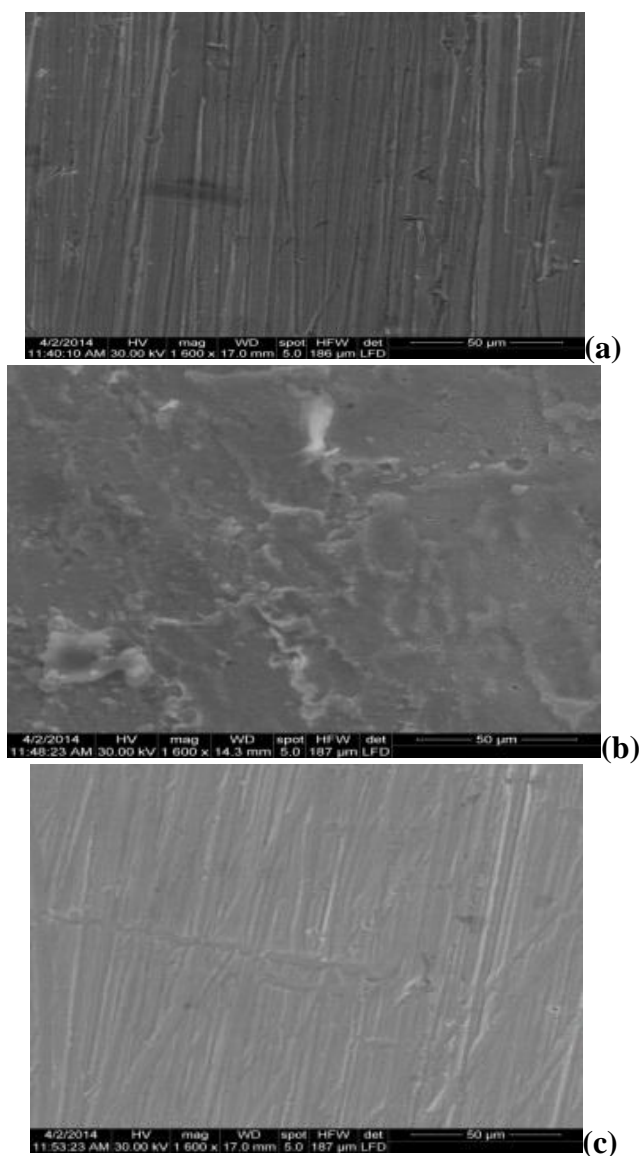


Fig. (12): SEM images for CaSO₄ formation in copper: a) polished sample, (b) after immersion in the sea water and (c) after immersion in the sea water in presence of inhibitor (III)

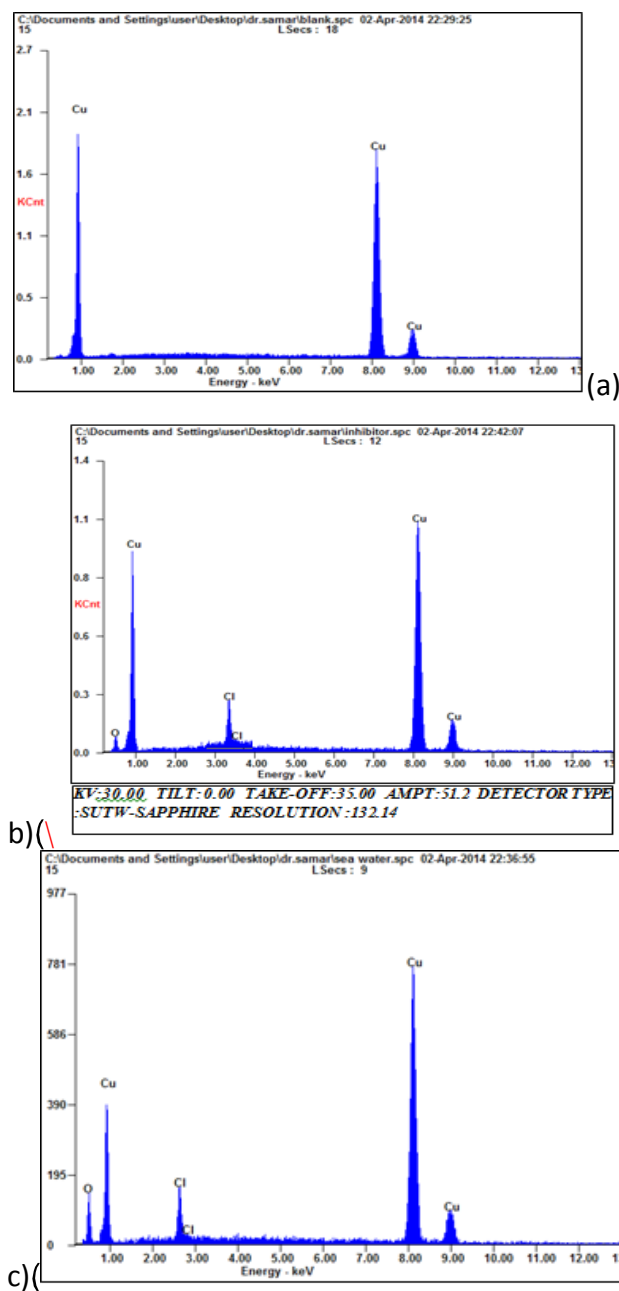


Fig. 13: EDX of the copper surface: (a) polished sample, (b) after immersion in the sea water and (c) after immersion in the sea water in presence of inhibitor (III)

Reference

- [1] F.K. Crundwell, *Electrochim. Acta* 37 (1992) 2101.
- [2] A. Dafli, B. Hammouti, R. Mokhlisse, S. Kertit, *Corros. Sci.* 45 (2003) 1619.

- [3] M. Abdallah, A.Y. Eletre, A.I. Mead, J. Electrochem. Soc. India 45 (1996) 71.
- [4] J. Mabrou, M. Akssira, M. Azzi, M. Zertoubi, N. Saib, A. Messaoudi, A. Albizane, S. Tahiri, Corros. Sci. 46 (2004) 1833.
- [5] D. Kuron, H.J. Rother, H. Graefen, Werkst. Korros.32 (1981) 409.
- [6] E. Geler, D.S. Azambuja, Corros. Sci. 42 (2000) 631.
- [7] L. Nunez, E. Reguera, F. Corvo, E. Gonzalez, C. Vazquez, Corros. Sci. 47 (2005) 461.
- [8] K.D.Demadis and S.D.Katarachia, Phosphorus,Sulfer,Silicon, 179 (2004) 627.
- [9] L.J.Simpson,Electrochim .Acta, 43 (16-17)(1998) 2543
- [10] J.C.Salmon,Polymer Materials Encyclopedia,CRC Press,Boca Raton, 1997, 7587 p.
- [11] W. Li, Q. He, C. Pei, B. Hov, Electrochim.Acta 52 (2007) 6386.
- [12] M. Stoll, R.D. Webster, J. Appl. Electrochem. 34 (2004) 225.
- [13] C. Wang, S. Chem, S. Zhao, J. Electrochem. Soc. 151 (2004) B11.
- [14] G. Kardas, Mater. Sci. 41 (2005) 337.
- [15] K.F. Khaled, N. Heberman, Electrochim. Acta 49 (2004) 485.
- [16] A.Y. El-Etre, M. Abdallah, Corros. Sci. 42 (2000) 731.
- [17] M. Abdallah, Corros. Sci. 44 (2002) 717.
- [18] J. Cruz, R. Martinez, J. Genesca and E. Garcia- Ochoa, Journal of Electro Analytical Chemistry, 566, 1, p. 111, (2004).
- [19] Daxi Wang, Shuyuan Li, Yu Ying, Mingjum Wang, Heming Xiao and Zhaoxu Chen, Corrosion science, 41, 10, P. 1911, (1999).
- [20] R.A. El-Ghazawy, Colloids Surf. A 260 (2005) 1–6.
- [21] X.H. Li, S.D. Deng, G.N. Mu, H. Fu, F.Z. Yang, Corros. Sci. 50 (2008) 420.
- [22] M.A. Migahed, M.A. Hegazy, A.M. Al-Sabagh, Corros. Sci. 61 (2012) 10.
- [23] Q.B. Zhang, Y.X. Hua, Electrochim. Acta 54 (2009) 1881.
- [24] A.P. Yadav, A. Nishikata, T. Tsuru, Corros. Sci. 46 (2004) 169.
- [25] K.F. Khaled, Appl. Surf. Sci. 252 (2006) 4120.
- [26] G. Saha, N. Kurmaih, Corrosion 42 (1986) 9.
- [27] I. Sekine, Y. Hirakawa, Corrosion 42 (1986) 272.
- [28] I. Sekine, T. Shimode, M. Yuasa, K. Takaoka, Ind. Eng. Chem. Res. 29 (1990) 1460.
- [29] P. Connor, R.H. Ottewill, J.Colloid interface Sci., 37 (1971) 642. The adsorption of cationic surface active agents on polystyrene surfaces
- [30] Suzuki, T., Kawamura, T., Corrosion and scale inhibitors for cooling water system, NACE, Houston, 1993.
- [31] Yasuda,M., Suzuki,K.,Kondo, Y.,Ogata,Y.,Hine,F., Corrosion 41,331,(1985).
- [32] ASTM E 45-87, vol. 11, ASTM, Philadelphia, PA, (1980) 125.

